Absolute Peak Efficiencies of a Coaxial Type Ge(Li) Detector for Gamma-Rays of 3 to 11 MeV

By

Michio TOMITA* and Kouya OGINO*

(Received March 28, 1975)

Abstract

The experimental determination of the absolute peak efficiencies of the 35 cc coaxial type Ge(Li) detector is described for 3 to 11 MeV gamma-rays. An improvement is made concerning the estimation of the absolute yield of gamma-rays emitted from the nuclear resonance reactions that were used as monoenergetic gamma-ray sources.

The full and two escape peak efficiencies were determined as functions of the gamma-ray energy and the source-detector distance.

1. Introduction

To investigate the gamma-ray spectra is one of the most important tools for studying excited states of nuclei. When a particle is captured by a nucleus, a compound nucleus is formed with an excitation energy of about 5 MeV or higher.

For gamma-rays of an energy above 3 MeV, the detection efficiency of a coaxial type Ge(Li) detector can be determined experimentally, rather than computationally, because the sensitive area of the coaxial Ge(Li) detector is not so simple as a NaI detector or as a planer type Ge(Li) detector, for that reason, the calculation becomes very complicated and expensive.

The absolute peak efficiencies $\eta_i(E_0, R)$ of a Ge(Li) detector for gamma-rays of energy E_0 at the distance R from the point source are expressed as

$$\eta_i(E_0, R)=C_i/N_t \qquad (i=0, 1, 2) \tag{1}$$

where N_t is the absolute total gamma-ray yield emitted to the over-all direction from the source, and C_0 the number of gamma-rays forming the full energy peak. C_1 and C_2 are those of gamma-rays forming the single and double escape peaks.

In order to determine the absolute peak efficiencies at an energy above 3 MeV,

* Department of Nuclear Engineering

gamma-rays emitted from the nuclear resonance reactions have been utilized, such as thermal neutron capture reactions[1~3] and proton capture reactions[4~6].

Since the response function of a NaI detector has not been determined exactly, especially at the lower half of the response function, the methods to measure the total gamma-ray yield heretofore have been uncertain.

Recently, the response function of a $3'' \times 3''$ NaI scintillator has become computable for any energies between 3 and 20 MeV, by making use of the table of energy deposition functions given by Berger and Seltzer[7].

In the present report, the experimental determination of the absolute peak efficiencies is described. Making use of the fact that the total number of gamma-rays entered in a NaI scintillator is obtainable by integrating the response function with respect to energy, an improvement is made concerning the estimation of the absolute yield of gamma-rays from the nuclear resonance reactions.

2. Experimental Procedures

i) Nuclear reactions as a gamma-ray source

Energetic protons were obtained by the 4 MV Van de Graaff accelerator of Kyoto University[8].

Deflected by the 90°-magnetic analyser, proton beams were focused on the target by the magnetic Q-lens through a defining slit of 2 mm in diameter.

Nuclear resonance reactions utilized for gamma-ray sources are listed in Table 1. The properties of these reactions have been investigated in detail by many authors and summarized by F. Ajzenberg-Selov and T. Lauritsen[9~13], and by P. M. Endt and C. Van der Leun[14].

Since the intensities of these gamma-rays are very dominant at the adopted proton energies, the peak region in the NaI spectrum covering the full energy peak and the escape peaks is isolated from those of the other gamma-rays. Their contributions to the peak region are rather precisely estimated and can be subtracted. The spectra of the NaI detector are shown in Fig. 1 for each

Table 1. Nuclear resonance reactions used as gamma-ray sources.

Reaction	E_p (MeV)	E_γ (MeV)	Target
$^{27}Al(p, \gamma)^{28}Si$	0.992	10.76	pure aluminium
$^{9}Be(p, \gamma)^{10}B$	0.992	7.48	pure beryllium
$^{19}F(p, \alpha\gamma)^{16}O$	0.7	6.14	LiF
$^{11}B(p, \gamma)^{12}C$	0.7	4.43	fine powder of boric acid
$^{9}Be(p, \alpha\gamma)^{6}Li$	2.53	3.56	
$^{12}C(p, \gamma)^{13}N$	0.48	2.37	pure carbon

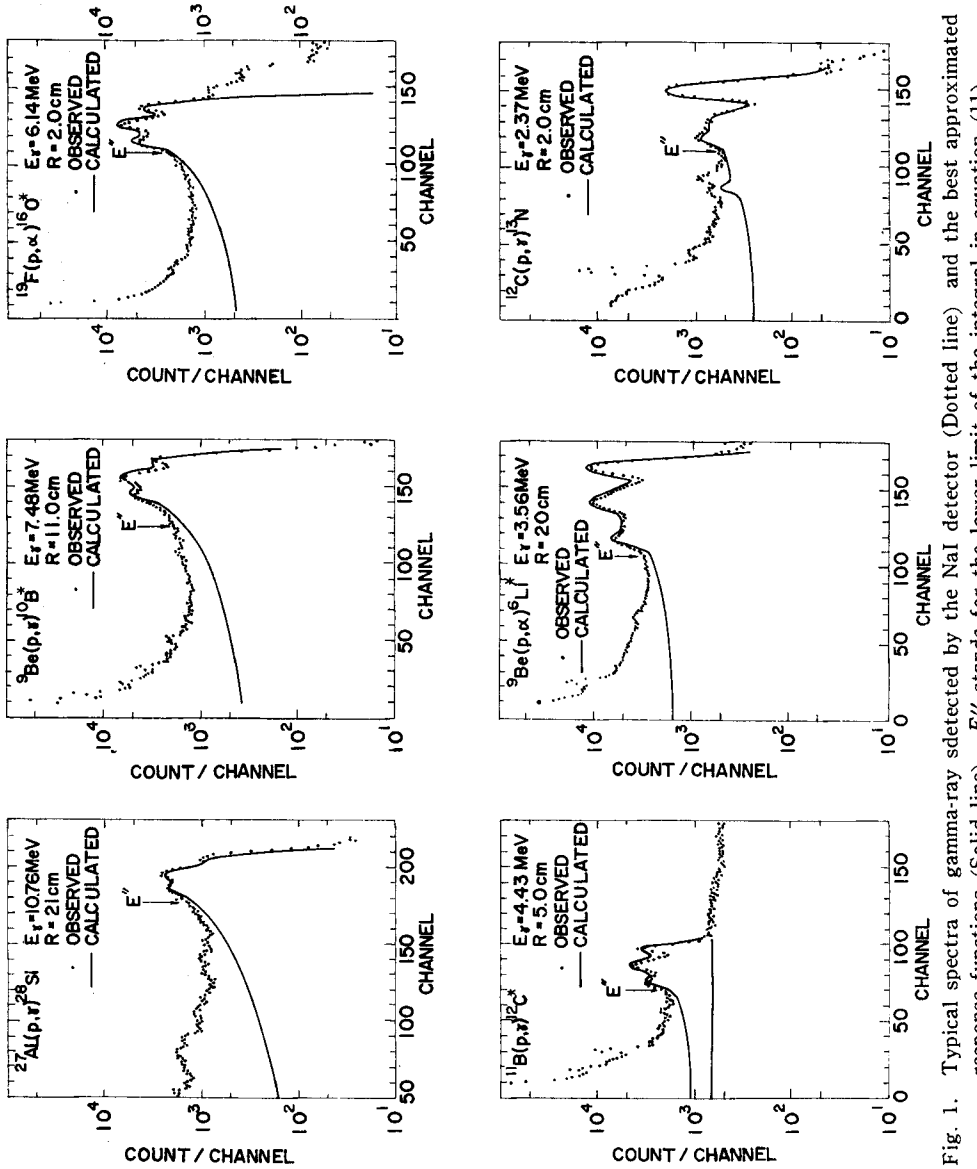

Fig. 1. Typical spectra of gamma-ray sdetected by the NaI detector (Dotted line) and the best approximated response functions (Solid line). E'' stands for the lower limit of the integral in equation (11).

gamma-ray energy.

ii) Targets

As the backing of the target, gold film about 10 μm was used. It was prepared by evaporation on a copper plate 1 mm thick, having two kinds of diameter, 2.0 cm and 0.3 cm respectively. The target with the smaller backing

plate was used when the source-detector distance* was very short, such as 0.5 cm and 1.0 cm. Two types of target chamber were used according to the size of the backing plates.

Aluminium and beryllium targets were prepared by evaporation. The boron target of natural abundance was prepared by mounting the fine powder of boric acid on the backing plate and covering it with a tantalum foil 3 μm thick. The fluorine target was prepared by dripping the colloidal volatile solution of lithium fluoride on the backing plate. The carbon target was prepared by the sputtering of pure graphite on the backing plate.

All the targets were thick ones, and were cooled by water when they were mounted on the target holder.

iii) Detectors

The Ge(Li) detector** used is a coaxial type one with 38.5 mm diameter and 34.5 mm length, mounted in an evacuated thin-wall aluminium container. The thickness of the front face of the container is 0.5 mm. The distance between the front face of the container and Ge(Li) crystal is 5 mm. The energy resolution

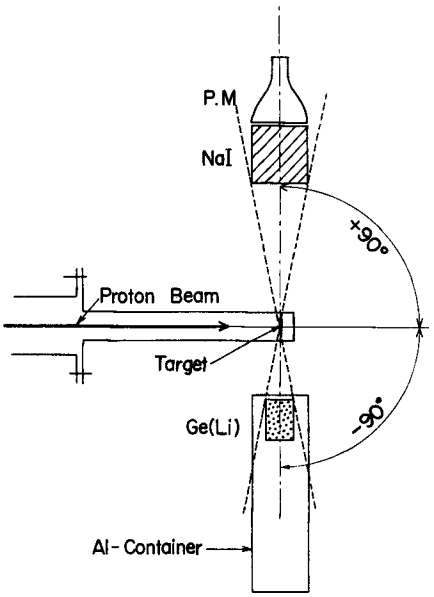

Fig. 2. Schematic diagram of the experimental arrangement. Velocity of the proton beam, centers of the NaI detector, and the Ge(Li) detector are in the same plane.

* "Source-detector distance" means the distance between the source and the front face of the detector container.

** This was purchased from ORTEC Incorporated, in U.S.A.

of the detector with 3000 V bias is 2.8 keV for 1.33 MeV gamma-rays from ^{60}Co.

The 3″×3″ NaI detector* was used to obtain the absolute gamma-ray intensity.

The experimental arrangement is shown in Fig. 2. The Ge(Li) and the NaI detectors were set at −90° and +90° with respect to the incident beam direction. They were located apart from the target center at distances to make both solid angles approximately the same so that no corrections were necessary for the angular distribution effects and the gamma-ray absorption in the target chamber. The measurements of gamma-rays were performed simultaneously with the Ge(Li) and the NaI detectors.

iv) Electronics

The Ge(Li) detector was operated at 3000 V bias. Being amplified by an ORTEC 120 preamplifier and an ORTEC 452 amplifier, signals from the Ge(Li) detector were fed to a Nuclear Data 4096-channel pulse height analyser.

The photomultiplier of DuMont-6363 was used for the NaI scintillator. Signals from the NaI detector were fed to a Nuclear Data 1024-channel pulse height analyser after an appropriate amplification by an ORTEC 113 prieamplifier and an ORTEC 440A amplifier.

During the measurements, the counting losses in the two pulse height analysers were kept within 2 %.

3. Absolute Yield of Gamma-Rays

For a NaI detector, the absolute total detection efficiency $\eta_t(E_0, R)$ at the distance R can be calculated by means of the Monte Carlo method[15]. If all of the signals that were generated by the gamma-rays of energy E_0 in the NaI detector placed at the distance R were counted and denoted N_s, the absolute total number of gamma-rays N_t emitted to the over-all direction could be expressed as

$$N_t = N_s/\eta_t(E_0, R). \tag{2}$$

For gamma-rays above 3 MeV, the response function of the NaI detector can be obtained only by calculation, since monoenergetic sources are lacking and background problems are usually severe. In the present report, the response functions were interpolated from the table of those given by Berger and Seltzer[7]. The response function agreed well with the observed spectra, being obtained in such a way that, only within the peak region of the spectra, the sum of the

* This was purchased from HORIBA, Ltd. in Japan.

square of the differences between the calculated and the observed spectra became minimum. This response function was integrated from the peak region to the zero energy of the continuum to obtain the total number of signals N_s.

According to the notation of Berger and Seltzer, the response function is written as

$$R(E_0, h) \propto \int_0^{E_0} D(E_0, E) G(E, h) dE \tag{3}$$

and

$$\int_0^{H_0} \int_0^{E_0} D(E_0, E) G(E, h) dE dh = 1 \tag{4}$$

where $D(E_0, E)$ and $G(E, h)$ represent the energy deposition function and the resolution function respectively. E_0, E, h, and H_0 denote an incident energy, an energy deposited to the detector, a pulse height arising from the deposited energy E, and the maximum pulse height due to the incident energy E_0 respectively. The energy deposition function $D(E_0, E)$ is rewritten as

$$\begin{aligned} D(E_0, E) = C(E_0, E) + P_0 \delta(E - E_0) + P_1 \delta(E - E_0 + mc^2) \\ + P_2 \delta(E - E_0 + 2mc^2) \end{aligned} \tag{5}$$

where δ is the delta function and $C(E_0, E)$ represents the continuum. P_0 is the probability that the entire energy E_0 is deposited in the detector. P_1 and P_2 are the probabilities that all of the energy is deposited, with the exception of the amounts mc^2 or $2mc^2$ being carried away by one or two unscattered annihilation quanta.

The normalization of the interpolated continuous part $C(E_0, E)$ was performed following the equation (4), being written as

$$k \int_0^{E_0} C(E_0, E) dE = 1 - \sum_j P_j \qquad (j = 0, 1, 2). \tag{6}$$

Using the constant k, the normalized continuum $C'(E_0, E)$ is

$$C'(E_0, E) = kC(E_0, E).$$

The energy resolution of the detector is defined as

$$r(W) = W(E)/E \tag{7}$$

wnere $W(E)$ is the full width at half maximum of the Gaussian. The resolution function is therefore written as

$$G(E, h) = (\alpha/\pi)^{1/2} \exp\{-\alpha(E_0 - h)^2\}, \tag{8}$$

where

$$\alpha=4\ln 2/\{r(E)E_0\}^2=4\ln 2/W(E)^2=1/(2\sigma E_0) \tag{9}$$

and σ is the standard deviation. Following the selection of Berger and Seltzer, the energy dependence of the resolution $r(E)$ was taken to be

$$r(E)=r(E')(E'/E)^{0.34}, \tag{10}$$

where E' denoted the reference energy that was chosen to be 0.661 MeV of the gamma-ray energy of ^{137}Cs.

Two parameters were used in order to obtain the response function $R^b(E_0, h)$ that agreed well with the observed spectra. They were the energy resolution of the detector and a factor K. K is defined as

$$K=S(E_0, h)/\int_{E''}^{E_0} D(E_0, E)G(E, h)dE, \tag{11}$$

where $S(E_0, h)$ is the observed spectrum of the peak region and E'' the energy

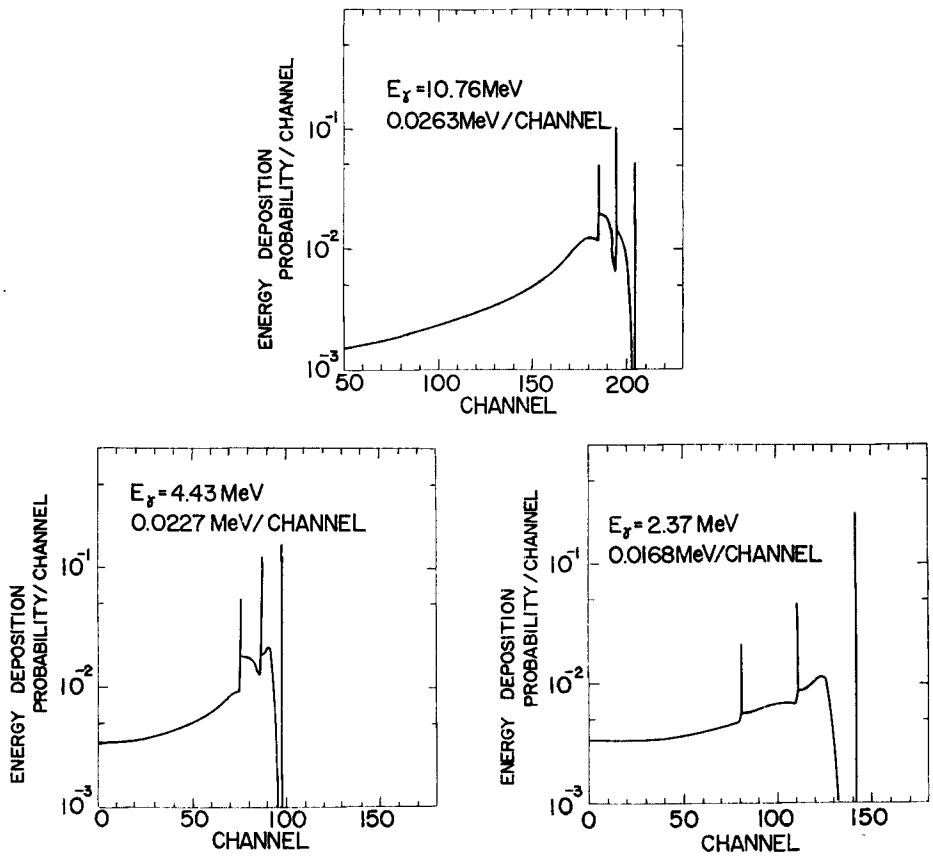

Fig. 3. Examples of the normalized energy deposition functions $D'(E_0, E)$ calculated by making use of the table given by Berger and Seltzer.

just below the lowest peak energy (see Fig. 1).

All of the detected gamma-rays N_s are therefore

$$N_s=\int_0^{H_0} R^b(E_0, h)dh, \tag{12}$$

where

$$R^b(E_0, h)=K_{opt}\int_0^{E_0} D'(E_0, E)G(E, h)dE \tag{13}$$

and

$$D'(E_0, E)=kC(E_0, E)+P_0\delta(E-E_0)+P_1\delta(E-E_0+mc^2) +P_2\delta(E-E_0+2mc^2). \tag{14}$$

The calculated response functions $R^b(E_0, h)$ are shown in Fig. 1 by the solid lines for every gamma-ray energy. The normalized energy deposition functions $D'(E_0, E)$ are shown in Fig. 3 for a few kinds of energies.

At the pulse heights below the peak region in Fig. 1, the observed spectra typically exhibit a rise to values that greatly exceed the calculated values. This rise has been explained as being due to the background from accompanying gamma-rays[4] and from those scattered by surrounding materials.

Berger and Seltzer estimated the relative standard deviation of the energy deposition functions to be 5, 8, 11, and 13 % for energies 1, 6, 12, and 20 MeV respectively. These are plotted as a function of the gamma-ray energy in Fig. 4.

Since the gamma-rays emitted from a nuclear reaction generally have an angular distribution, the value of N_s obtained in this way stands for the averaged

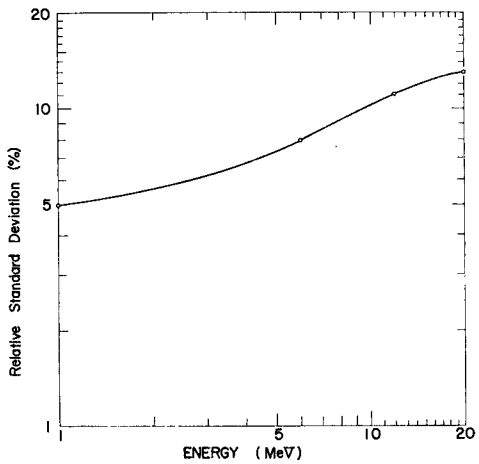

Fig. 4. Relative standard deviation as a function of the gamma-ray energy.

value over the solid angle sustained by the NaI detector.

The absolute total detection efficiency $\eta_t(E_0, R)$ was calculated by using the Monte Carlo calculation code REFUM[15] for every incident energy E_0 and source-detector distance R. The obtained values of $\eta_t(E_0, R)$ are in good agreement with those interpolated from the curves given by Marion and Young[16]. They are shown at the third column in Table 2.

Table 2. The calculated and observed numbers for each gamma-ray energy and source-detector distance.

E_0 (MeV)	R (cm)	η_t	N_s $\times 10^4$	N_t $\times 10^4$	C_0	C_1	C_2
2.37	0.5	0.09506	6.94	7.30	2199	271	670
	1	0.06731	5.62	8.35	1582	195	505
	2	0.03778	4.45	1.18	1609	260	597
	5	0.01225	1.91	1.56	619	113	219
	10	0.004174	1.06	2.54	420	62	125
3.56	0.5	0.08920	64.2	7.20	10513	4711	10980
	1	0.06231	49.4	7.93	7723	3432	8434
	2	0.03584	46.4	16.5	10391	4867	10915
	5	0.01169	17.5	15.0	3476	1444	3533
	10	0.003921	20.9	53.3	3565	1418	3793
4.43	0.5	0.08856	10.5	1.18	938	742	1842
	1	0.06238	7.43	1.19	808	576	1386
	2	0.03482	12.3	6.24	2872	2177	5101
	5	0.01143	9.01	7.88	1061	828	1876
	10	0.003895	6.01	15.4	753	492	1351
6.14	0.5	0.08792	24.1	2.74	1486	2087	5005
	1	0.06147	25.9	4.21	1705	2362	5366
	2	0.03498	39.5	12.0	2619	3918	10137
	5	0.01136	20.1	17.7	1677	2098	4679
	10	0.003916	5.01	12.8	382	460	1061
7.48	0.5	0.08909	22.2	2.49	888	1714	4170
	1	0.06284	28.2	4.49	961	1863	4697
	2	0.03546	78.9	24.9	3853	7882	17693
	5	0.01156	25.2	21.8	925	1857	4495
	10	0.003925	25.2	64.2	889	1926	4346
10.76	0.5	0.09130	40.5	4.44	510	2032	13567
	1	0.06432	55.9	8.69	651	2754	7007
	2	0.03627	54.5	8.27	462	2059	4622
	5	0.03627	9.66	8.21	176	671	1425
	10	0.00400	11.0	27.5	132	668	1557

Finally, following the equations (2) and (12), the absolute gamma-ray yield N_t was calculated for each case of the observations. The values of N_t are tabulated at the fifth column in Table 2, associated with the numbers C_0, C_1, and C_2.

4. Results and Discussion

Following the equation (1), the absolute peak efficiencies, $\eta_0(E_0, R)$, $\eta_1(E_0, R)$, and $\eta_2(E_0, R)$ of the 35 cc Ge (Li) detector were obtained. They are shown in

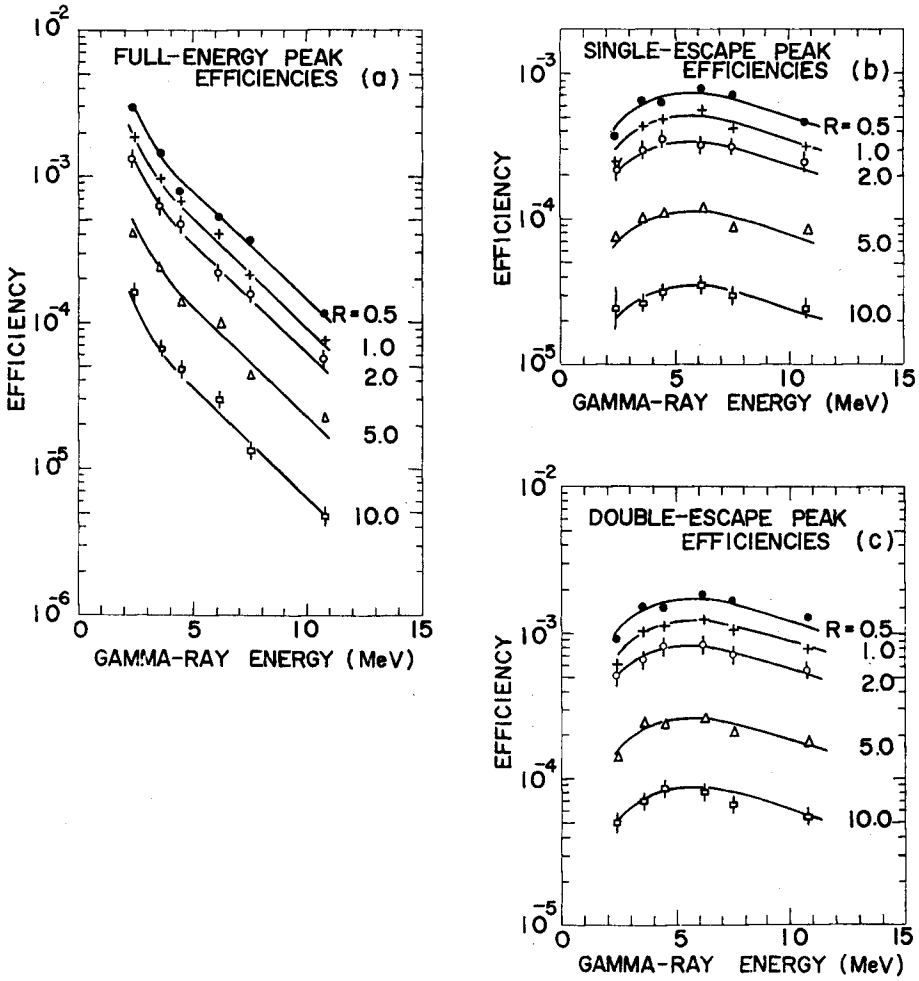

Fig. 5. Absolute peak efficiencies as a function of the gamma-ray energy. R denotes the source-detector distance. Solid lines represent the best approximated curves for each source-detector distance. (a) Full energy peak efficiencies, (b) Single escape peak efficiencies, (c) Double escape peak efficiencies.

Fig. 5(a), (b), and (c) respectively. The trend that every curve in Fig. 5(b), and (c) has the maximum at about 6 MeV, is attributed to the effect that the probability of the energy loss, by the bremsstrahlung of the electron produced in the germanium crystal, becomes greater as the gamma-ray energy increases above 6 MeV.

The errors of the peak efficiencies shown in Fig. 5 are the standard deviation. The error attributed to the response function was estimated from the curve in Fig. 4. In almost all cases it was more dominant than the standard deviation of the observed spectra. With the exception of a few cases of the 2.37 MeV gamma-ray, the resulting error of the peak efficiencies is at most 12 % for the 10.76 MeV gamma-ray, and is even less than that for the lower energy gamma-rays.

The values of the ratio $\eta_2(E_0)/\eta_1(E_0)$ are shown in Fig. 6 as the function of gamma-ray energy for each source detector-distance. It is natural consequence that the ratio $\eta_2(E_0)/\eta_1(E_0)$ has a constant value (in the present case, it is 2.4) with an experimental accuracy independent of the gamma-ray energy E_0 and the source-detector distance R, if the procedure by which escape peaks appear is taken into account. In the semi-logarithmic scale, the curve of $\eta_2(E_0)$ should therefore have the same shape as that of $\eta_1(E_0)$.

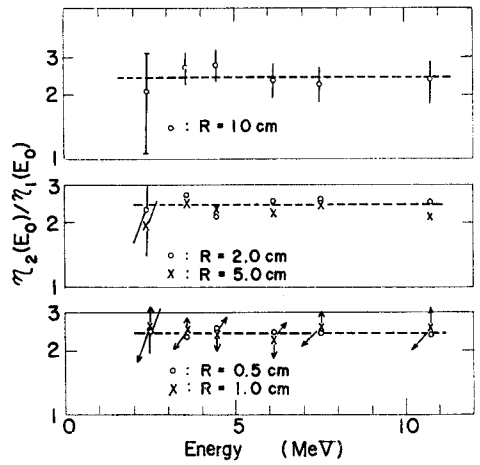

Fig. 6. Ratio of the double escape peak efficiency $\eta_2(E_0)$ to the sigle escape peak efficiency $\eta_1(E_0)$ for each case of the source-detector distance. Broken line represents the value averaged over all of the ratio.

The solid lines in Fig. 5(a), (b), and (c) represent the best approximated curves of $\eta_0(E_0, R)$, $\eta_1(E_0, R)$, and $\eta_2(E_0, R)$ respectively

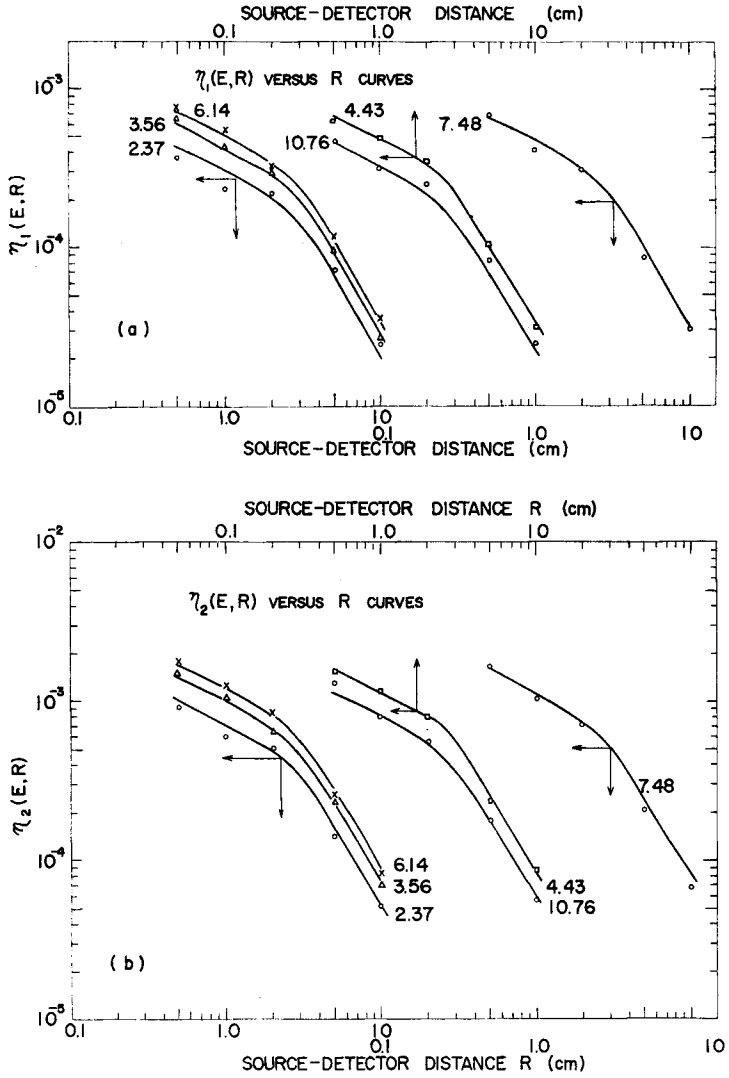

Fig. 7. $\eta(R)$ vs. R curves, (a) for the single escape peak efficiencies and (b) for the double escape peak efficiencies. Figures by the curves stand for the gamma-ray energy.

From the fact that the ratio $\eta_2(R)/\eta_1(R)$ is also constant, the $\eta_2(R)$ curve should have the same shape as that of $\eta_1(R)$ for each gamma-ray energy $\eta_1(R)$ and $\eta_2(R)$ are plotted as a funnction of the source-detector distance R for each gamma-ray energy in Fig. 7(a) and (b) respectively. The solid lines in Fig. 7 were obtained from those in Fig. 5(b) and (c). Evidently, the value of $\eta_1(R)$ or $\eta_2(R)$ is proportional not to $1/R^2$ but approximately to $1/R^{0.5}$ between 0.5 cm

and 3.0 cm, and to $1/R^{1.6}$ between 3.0 cm and 10.0 cm. This may be attributed to the fact that the significant solid angle sustained by Ge (Li) detector is not proportional to $1/R^2$ by reason of the complex form of the sensitive area.

Using the cusves in Fig. 5 and Fig. 7, one can obtain at once the curves of the absolute detection efficiencies for the escape peaks of this Ge(Li) detector at any source detector distance less than 10 cm.

Acknowledgments

The authors would like to express their thanks to Dr. T. Nakamura for his valuable advice concerning the Monte Carlo code REFUM. The collaborations of Messrs. M. Yoshioka, Y. Okataku, S. Hayashi, and Y. Kadota are gratefully acknowledged. Further thanks are extended to Professor T. Nishi and his collaborators of the Institute of Atomic Energy for valuable advice and help in the target preparation of beryllium. The numerical calculations in this work were made at the Data Processing Center of Kyoto University.

References

1) J. E. Cline: IEEE Trans. Nucl. Sci., NS-15, 198 (1968).
2) W. R. Kane and M. A. Mariscotti: Nucl. Instr. & Meth., **56**, 189 (1967).
3) J. Kopecky, R. W. Ratynski and E. Warming: Nucl. Instr. & Meth., **50**, 333 (1967).
4) J. Kockum and N. Starfelt: Nucl. Instr. & Meth., **4**, 171 (1959).
5) R. Nordhagen: Nucl. Instr. & Meth., **12**, 291 (1961).
6) F. C. Young, A. S. Figuera, and G. P. Feufer: Nucl. Inst. & Meth., **92**, 71 (1971).
7) M. J. Berger and S. M. Seltzer: Nucl. Instr. & Meth., **104**, 317 (1972).
8) F. Fukuzawa, et al.: THIS MEMOIRS, **35**, 52 (1973).
9) F. Ajzenberg-Selov and T. Lauritsen: Nucl. Phys., **11**, 1 (1959).
10) F. Ajzenberg-Selov: Nucl. Phys., **A152**, 1 (1970).
11) F. Ajzenberg-Selov: Nucl. Phys., **A166**, 1 (1971).
12) F. Ajzenberg-Selov: Nucl. Phys., **A190**, 1 (1972).
13) F. Ajzenberg-Selov and T. Lauritsen: Nucl. Phys., **A227**, 1 (1974).
14) P. M. Endt and C. Van der Leun: Nucl. Phys., **A214**, 1 (1973).
15) T. Nakamura: Nucl. Instr. & Meth., **105**, 77 (1972).
16) J. B. Marion and F. C. Young: "Nuclear Reaction Analysis, graphs and tables", North-Holland Publishing Co., Amsterdam, p. 48 (1968).